Temporal Evolution of X and C Band SAR Backscattering in theMont-Blanc Massif

Suvrat Kaushik, Matthieu Gallet, Yajing Yan, Abdourrahmane Atto, Ludovic Ravanel, Emmanuel Trouvé

TEMPORAL EVOLUTION OF X AND C BAND SAR BACKSCATTERING IN THE MONT-BLANC MASSIF

Suvrat Kaushik[1,2], Matthieu Gallet[1], Yajing Yan[1], Abdourrahmane Atto[1], Ludovic Ravanel[2], Emmanuel Trouvé[1]

1. LISTIC, Université Savoie Mont-Blanc, Annecy, France
Contact : {firstname.lastname}@univ-smb.fr
2. EDYTEM, CNRS - Université Savoie Mont-Blanc, Le Bourget du Lac, France

ABSTRACT

In this paper, two SAR image time series acquired by PAZ and Sentinel-1 satellites in 2020 (29 and 60 images respectively) are used to investigate surface changes of different ice/snow-covered areas in the Mont-Blanc massif. The evolution of the backscatter coefficient and several statistical parameters in both X and C band SAR images is analyzed on ice aprons, on valley glacier accumulation and ablation areas, and on ice-free areas. Dry and wet snow changes are observed and correlated with meteorological data (temperature at 4 different elevations and snow height) acquired by a weather station.

***Index Terms*—** SAR, X/C bands, Snow/Ice backscatter

1. INTRODUCTION

The Sentinel-1 6-day repeat pass acquisitions over Europe has created image time series where the temporal evolution of the radar backscatter can be observed in the C-band at about 10 m resolution. Higher-resolution images can also be obtained in X-band from commercial satellites such as TerraSAR-X and PAZ. Both sources of multi-temporal SAR images are particularly interesting in monitoring snow and ice-covered regions and analyzing their evolution. SAR backscattering signals from snow/ice depend on snowpack or ground characteristics, which include the temperature, density, liquid water content, the size and shape of the particles, and surface roughness. Hence the backscatter evolution analyzed from the SAR repeated acquisitions can provide valuable information about the physical state of the feature under study. In this paper, two SAR image time series from PAZ and Sentinel-1 satellites are used to investigate surface changes of different ice/snow-covered areas in high mountain regions. The evolution of the backscatter coefficient and statistical parameters in both the X and C band SAR image time series is analyzed on the following features:

- Ice Aprons (IAs), which are 'extremely small' (generally < 0.009 km^2 for the Mont-Blanc massif) and thin ice patches of irregular shape, existing above the regional Equilibrium Line Altitude (ELA) on very steep slopes (generally between 40 and $65°$) [1];
- Valley glaciers with their accumulation areas where snow transforms into firn and ice, and their ablation areas with bare ice after snow melt [2];
- Ice-free areas where dry then wet snow creates scattering changes which can be used to map snow-covered areas [3].

2. STUDY SITE & DATASET

The study area for the analysis is the Mont-Blanc massif (MBM) (Figure 1). The massif occupies 550 km^2 spread across France, Switzerland, and Italy. Glaciers cover about 145 km^2, thus making it the highest and most glacierized massif in the French Alps. The geology and the complex topography of the terrain, combined with long periods of glacial erosion, provide relevant conditions for the development of various snow/ice features.

To understand the temporal evolution of the above-mentioned features, we present an analysis and a comparison of one year of Sentinel-1 regular acquisitions and of PAZ acquisitions between January 08, 2020, and December 30, 2020. All images of PAZ are dual-polarization (HH/HV) acquired at 5h44 AM over the study area in descending orbits with an incidence angle of 37.8° and every 11 days. Sentinel-1 images were acquired at 05h35 AM every 6 days with a nominal incidence angle of 38.3° and are also in dual-polarization but with vertical emission polarization (VV/VH). The main difference is the operating frequency of each satellite. While Sentinel-1 works in C-band with a center frequency of 5.405 GHz, PAZ operates in X-band with a center frequency of 9.65 GHz and a larger bandwidth, which has a direct impact on the image resolution of each satellite: around 10 m for Sentinel-1 versus 3 m for PAZ. This difference in frequency also affects the wave's ability to penetrate an environment, particularly in the presence of water. In this way, C-band satellites are able to detect wet snow, while X-band satellites have more often been used to determine snow depths [4] and glacier speeds. Images from both satellites cover almost the whole

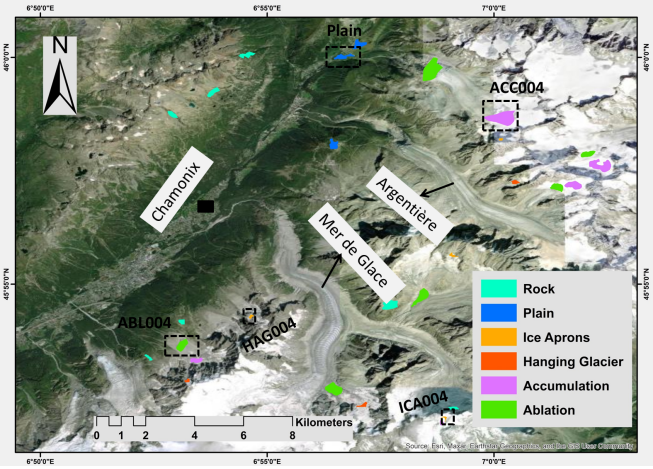

Fig. 1: The study site (Mont-Blanc massif, Western European Alps). ACC004, ABL004, HAG004, and ICA004 denote the locations of the respective classes for which the statistical analysis is presented in Figure 3. The location of the plain area over which the analysis shown in Figure 2 was performed is also marked.

study region, allowing the selection of different areas spread across the massif with different topographic characteristics. This gives us two time series of 29 and 60 images for the PAZ and Sentinel-1 satellites respectively.

3. METHODOLOGY

Basic pre-processing steps (i.e. coregistration, radiometric calibration, and normalization) for the entire time series were performed in ENVI SARScape software. Geocoding of the images was however not performed, to avoid errors generated from the utilized DEM. Hence the entire analysis was performed on SAR images in their original slant-range geometry. We propose to compare the average backscatter coefficient of the C-band as a function of the X-band, for a selection of 4 glacier objects, with respect to the temporal evolution to better understand these bodies' evolution over time. In order to make this comparison, we first perform a temporal interpolation on the outer join of the X and C band series. We use derivative interpolation in order to obtain a smooth signal without steps. We propose in a second step to compare the correlations between meteorological measurements and a set of statistics based on the backscatter coefficient for each band (X and C). For the physical measurements, we use meteorological data from sensors of a single weather station provided by CREA: in the MBM, and located on an open plain at approximately 1400 m a.s.l. The plain represents an open area of short grass, a few scattered bushes, and no forest, as indicated in Figures 1. The station provides daily snow height and temperature information at 4 different elevations: 2 m and 0.3 m above ground, at ground level, and at 0.3 m depth. We have selected two important periods in alpine environments in view of the radar information [5], the one when the snow present is mainly dry and has little liquid water content (December, January, and February 2020), and the one when the more important presence of liquid water in the snowpack makes the snow wet (March, April and May 2020). The idea is to focus on a relatively stable area over time (open field) in order to see which statistics of the SAR signal, and the meteorological measurements are most correlated. The proposal to separate the data between 2 periods stems from the sensitivity of the radar signal to snowpack moistening. We studied the Spearman correlation coefficient between these physical measurements and several statistical parameters in both C and X bands as described in Table 1. This coefficient allows a correlation to be quantified even in the case of a non-linear relationship, and it is given by:

$$r_s = \frac{\mathrm{cov}(\mathrm{R}(X), \mathrm{R}(Y))}{\sigma_{\mathrm{R}(X)}\sigma_{\mathrm{R}(Y)}},$$

where $\mathrm{R}(\cdot)$ denotes the operator giving the rank of the variable, $\mathrm{cov}(\cdot)$ the covariance and σ the standard deviation. In order to consider the reliability and relevance of the correlation coefficient, we studied the associated p-value (probability value). The p-value corresponds to a hypothesis test where the null hypothesis states that there is no linear correlation between two sets of data. Typically, a value with a p-value < 0.05 is considered to have strong evidence against the null hypothesis. It is common to consider that a p-value > 0.1 does not provide any evidence for or against the null hypothesis.

Name	Description
mean_*XX*[1]	Mean backscattering coefficient
std_*XX*	Standard deviation of backscattering coefficient
CV_*XX*	Coefficient of variation (reveals the presence of heterogeneity within the estimation window [6])
skew_*XX*	Skewness of backscattering coefficient
kurt_*XX*	Kurtosis of backscattering coefficient
k1_*XX*	First log-cumulant of the distribution of backscattering coefficient [7]
k2_*XX*	Second log-cumulant of the distribution of backscattering coefficient
k3_*XX*	Third log-cumulant of the distribution of backscattering coefficient
T°-30cm	Temperature at 30 cm depth
T°0cm	Temperature at surface
T°30cm	Temperature at 30 cm above the ground
T°200cm	Temperature at 200 cm above the ground
height	Height of the snow layer
DS_day	Snow depth difference between the day of satellite acquisition and the day before
DS_SAT	Snow depth difference between two satellites acquisition[2]

Table 1: Description of the physical variables studied and the statistics calculated for each band.

[1] Polarisation: HH or HV for X-band data and VV or VH for C-band data
[2] ∼11 days for PAZ data (X-band), ∼6 days for Sentinel-1 data (C-band)

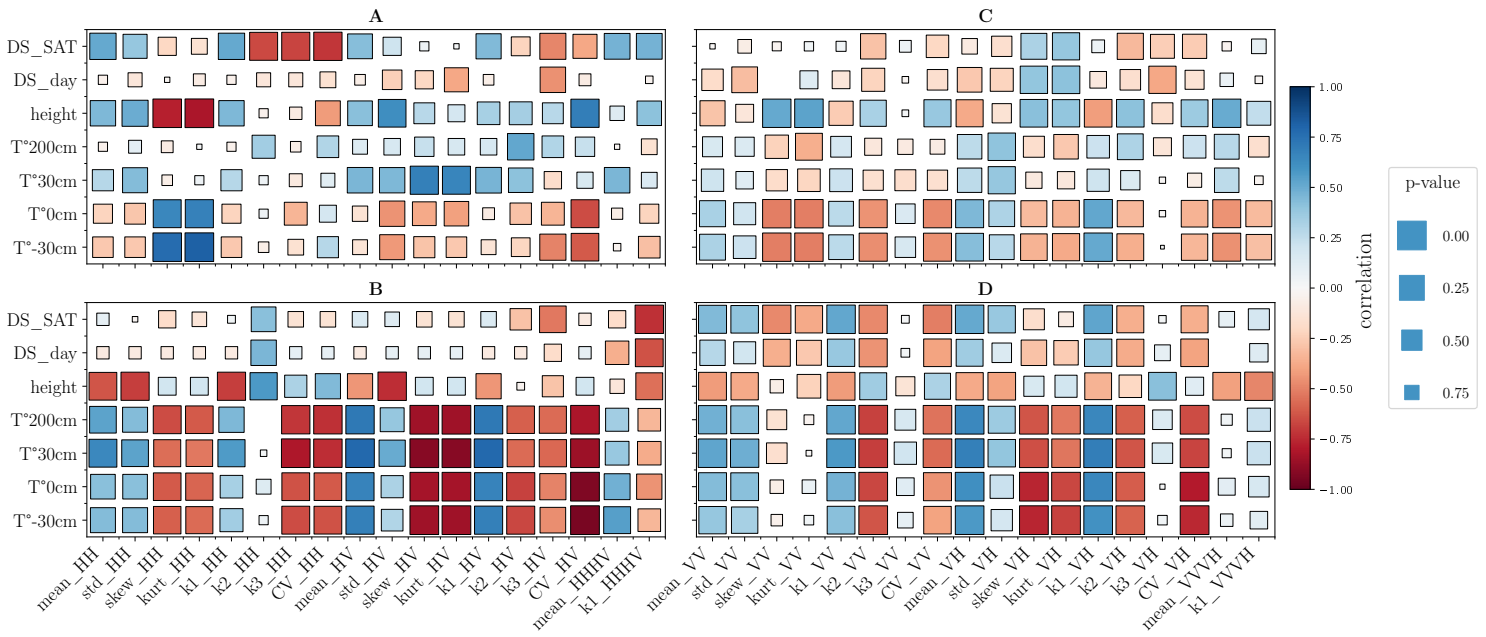

Fig. 2: Figures A and B represent the correlation tables between the physical measurements of temperature, height, and snow height difference and a set of statistics from the X-band backscatter coefficient (PAZ). Figures C and D represent the same correlations but with statistics from the C-band backscatter coefficient (Sentinel-1). The first line (Figure A and C) gives the correlations for a period of mostly dry snow (December, January, and February 2020). The second line (Figures B and D) gives the correlations for a period of mainly wet snow (March, April, and May 2020).

4. RESULTS

Figures 2 **A** and **B** proposes an analysis of the correlations between physical measurements obtained by meteorological data and statistics calculated over a plain area in the X-band, while Figures 2 **C** and **D** offer the same view but with C-band data over the same area. The different physical measurements and statistics are summarized in Table 1. While the first line (Figures 2 **A** and **C**) gives the correlations of the statistics of the two bands (X and C) for a period (December, January, and February 2020) when the snow present in the mountains is mainly low in liquid water content (i.e. dry snow), the second line (Figures 2 **B** and **D**) gives the correlations for a period (March, April, and May 2020) when the liquid water content is higher and the presence of snow at this period can be mainly associated with wet snow. This period distinction is important because radar radiation is sensitive to the presence of water in the snowpack. The quality of the correlation obtained is given by the p-value represented by the size of the squares.

A strong anti-correlation of the X-band signal with temperature is observed thanks to the 3rd (skewness) and 4th-order (kurtosis) statistics for the HV channel during the melting period. This indicates a decrease in backscatter values with an increase in temperature leading to an increase in the liquid water content of the snowpack. Similarly, we can see a certain sensitivity (positive or negative correlation) of the snow height to the CV. Variation of spatial CV values is an indicator of an increase in surface heterogeneity. An association of CV values with snow height could be a good indicator of surface melting. More generally, we note that X-band statistics are strongly correlated (positively or negatively) with different temperatures during the melt period. It is interesting to note that there is a correlation between periods of dry snow and direct or derived (snow difference) information on snow height, whereas in C-band the correlations are weaker, which can be explained by the fact that the snowpack is more transparent in C-band when the snow is dry. On the other hand, the C-band snowmelt correlates more strongly than the X-band snow height variables. It is interesting to see that in both bands there is a strong correlation between the radar signal and temperatures when the snow is not wet. Figure 3 shows the relationship between the C and X band backscatter averages for four classes of glaciers and perennial snow ice features (IA, hanging glacier, ablation area, and accumulation area). A linear relationship between X-band and C-band for all the classes is observed, which shows a similarity in the evolution trends of all classes in both bands. A more detailed analysis to understand the subtle differences between the backscatter response in the two bands should be performed in the future.

Further, the evolution of the backscattering coefficient of the snow is strongly related to the meteorological conditions, with a decrease when snow becomes wet. The behaviour is similar in X and C bands, but differences in the degree of attenuation can be observed in different areas. More differences are observed in IAs, which also present an increase in the CV values in the summer months, probably related to an increase

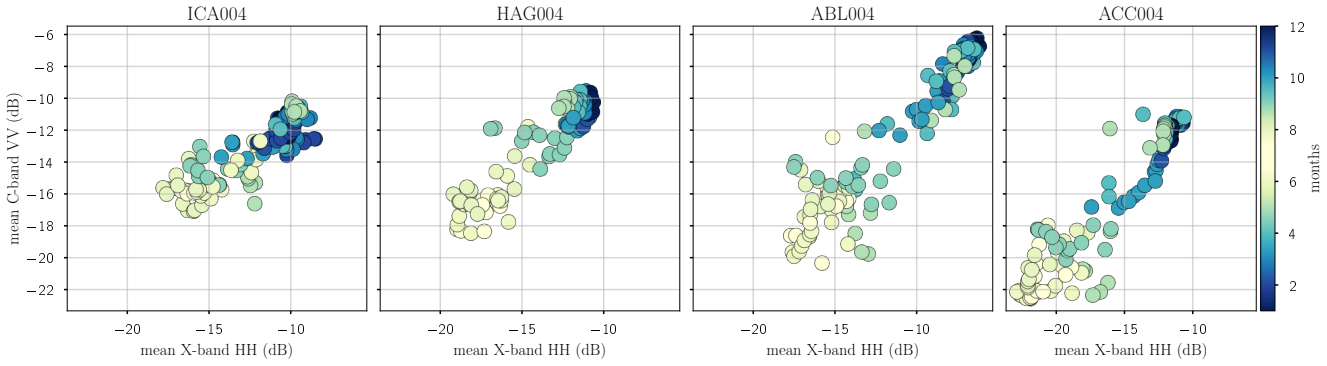

(a) co-polarization case

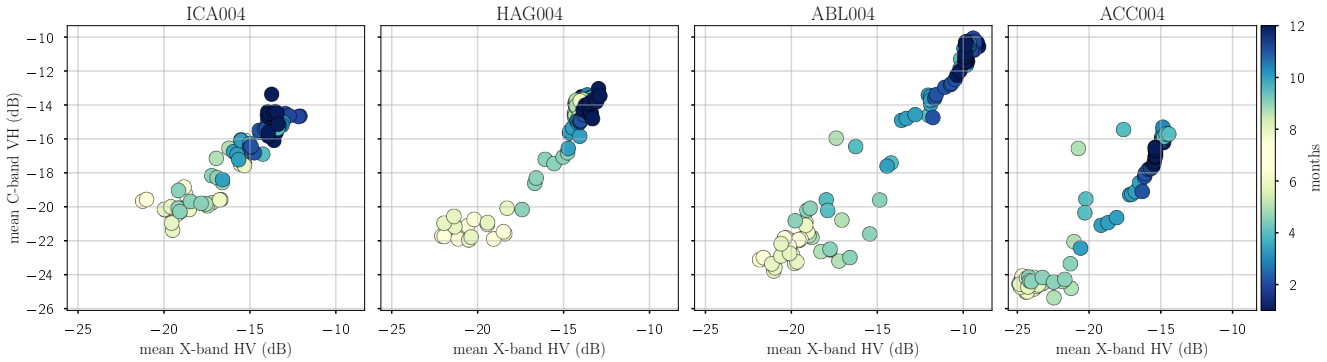

(b) cross-polarization case

Fig. 3: Comparison between the mean X and C band backscatter coefficient for 4 classes over a full year using interpolation.

in surface heterogeneity. This can result from the exposure of rock and ice with rocky debris on the surface of IAs after an extended period of intense melting.

5. CONCLUSIONS

As observed through the SAR image time series, the temporal evolution of different land classes provides valuable information about their physical properties. This further highlights the potential of using SAR images even in complex mountain topographies. The slight differences in their evolution, as observed through backscattering changes, can be used for automatic classification techniques in the future to differentiate different ice bodies.

Acknowledgement The authors would like to thank the *Spanish Instituto Nacional de Tecnica Aerospacial* (INTA) for the PAZ images (Project AO-001-051) and the *Centre de Recherches sur les Écosystèmes d'Altitude* (CREA) for the *in-situ* measures. The work was conducted as part of the SHARE CNES/PNTS project.

6. REFERENCES

[1] Suvrat Kaushik, Ludovic Ravanel, Florence Magnin, Emmanuel Trouvé, and Yajing Yan, "Ice aprons in the mont blanc massif (western european alps): Topographic characteristics and relations with glaciers and other types of perennial surface ice features," *Remote Sensing*, vol. 14, no. 21, 2022.

[2] Suvrat Kaushik, Bastien Cerino, Emmanuel Trouve, Fatima Karbou, Yajing Yan, Ludovic Ravanel, and Florence Magnin, "Analysis of the temporal evolution of ice aprons in the mont-blanc massif using X and C-band SAR images," *Frontiers in Remote Sensing*, vol. 3, 2022.

[3] Fatima Karbou, Gaëlle Veyssière, Cécile Coleou, Anne Dufour, Isabelle Gouttevin, Philippe Durand, Simon Gascoin, and Manuel Grizonnet, "Monitoring wet snow over an alpine region using sentinel-1 observations," *Remote Sensing*, vol. 13, no. 3, 2021.

[4] Silvan Leinss, Giuseppe Parrella, and Irena Hajnsek, "Snow height determination by polarimetric phase differences in x-band sar data," *IEEE Journal of Selected Topics in Applied Earth Observations and Remote Sensing*, vol. 7, no. 9, pp. 3794–3810, 2014.

[5] T. Nagler and H. Rott, "Retrieval of wet snow by means of multitemporal SAR data," *IEEE Transactions on Geoscience and Remote Sensing*, vol. 38, no. 2, pp. 754–765, 2000.

[6] Elise Colin Koeniguer and Jean-Marie Nicolas, "Change detection based on the coefficient of variation in SAR time-series of urban areas," *Remote Sensing*, vol. 12, no. 13, 2020.

[7] Jean-Marie Nicolas and Stian Normann Anfinsen, "Introduction to second kind statistics: Application of log-moments and log-cumulants to the analysis of radar image distributions," *Trait. Signal*, vol. 19, no. 3, pp. 139–167, 2002.